

A THM coupled distinct element model for simulating hydraulic fracturing in discontinuum reservoir with application to enhanced geothermal system

Botong Du

*Department of Geotechnical Engineering, College of Civil Engineering, Tongji University, China
(dubotong@tongji.edu.cn)*

Fengshou Zhang

Department of Geotechnical Engineering, College of Civil Engineering, Tongji University, China

Chongyuan Zhang

Institute of Geomechanics, Chinese Academy of Geological Sciences, China

Abstract

This study presents a three-dimensional thermal-hydro-mechanical (THM) coupled modeling workflow using the distinct element method to simulate fluid flow in fractured rock reservoirs. The model employs full hydro-mechanical coupling to assess the injection-induced responses of the reservoir, including the initiation and propagation of fractures, with natural fractures being explicitly represented through a discrete fracture network (DFN). Temperature calculations consider heat conduction within the reservoir and heat convection at the fracture surface, with thermal implications for stress and fluid properties. The numerical model performs stable iterative computations. A hydraulic fracturing simulation is produced based on the data from the Gonghe enhanced geothermal system (EGS) site in northwest China, followed by the study of the thermal effects on flow behavior. The results show that the rate of fracking in the THM model is faster than the HM model in the early stage. Cold water injection promotes fracture damage, but the effects diminish with time. Fluid viscosity decreases with increasing temperature, which can be detrimental for fluid to frack and prop fractures. By adjusting fluid viscosity and injection rate, the effect of temperature on cracking can be more effectively exploited. This research offers an approach to multi-field coupling in fractured rock masses, aiding in designing and assessing EGS and similar projects.

Keywords

Hydraulic fracture, Distinct element model, THM, DFN, Enhanced geothermal system

1 Introduction

Fluid injection induces complex reservoir responses in unconventional energy extraction and sequestration projects (Schimmel et al. 2019). As depth increases, temperature emerges as a critical factor that cannot be ignored. High-temperature and high-pressure conditions significantly alter fluid properties and rock stress states, consequently influencing the effectiveness of hydraulic fracturing and the associated risks (Li et al. 2024). Therefore, incorporating thermal effects into multi-field coupling has become increasingly essential for accurate simulations and risk assessments.

Fractures are prevalent in the development sites of hot dry rock, shale oil, and gas reservoirs (Yuan & Wood 2018). Existing studies have demonstrated that the behavior of natural fractures plays a decisive role in determining the stimulation performance of reservoirs (Riahi et al. 2019). Introducing natural fractures into hydraulic fracturing numerical models enables a more precise simulation of reservoir responses, improving the predictive capacity of such models.

Current simulation methods for evaluating the thermal effects in fractured reservoirs largely rely on simplified or implicit representations of fractures (Liao et al. 2023, Xue et al. 2023, Liu et al. 2024). It is still a lack of adequate analysis for fluid flow and stress evolution along fracture surfaces. Consequently, there is a pressing need to develop advanced modeling techniques capable of simulating fracture behavior under multi-field coupling, thereby addressing the limitations of existing methods.

This study focuses on the Gonghe Basin, a key geothermal development site in northwestern China, as the research background. The dry heat rock body discovered in the Gonghe Basin has the highest bottomhole temperature of 236°C with a depth of less than 4000 m (Zhang et al. 2018). Using the distinct element method, a thermal-hydro-mechanical (THM) coupled simulation workflow is developed to model fluid injection while explicitly accounting for natural fractures. This approach advances the understanding of reservoir responses under thermal effects and offers practical insights for optimizing hydraulic fracturing in high-temperature reservoirs.

2 Methodology

2.1 Numerical method

A three-dimensional distinct element method is adopted in this study to simulate the response of discontinuous reservoirs (3DEC, Itasca Consulting Group, Inc. 2016). In this method, the reservoir is pre-divided into irregular fractured rock bodies. The interior of the rock mass is divided into a tetrahedral finite-difference mesh. The discontinuous jointed surfaces between the rock masses are regarded as the boundaries of the rock body and provide paths for fluid flow.

Discrete fracture networks (DFN) are used to explicitly characterize natural fractures in reservoirs. The orientation and density distribution characteristics of reservoir fractures are obtained from drilling data in the field, and power law distribution is applied to set the fracture size. The primary fracture plane utilized in hydraulic fracturing is established as a pre-joined vertical plane aligned with the maximum horizontal principal stress and is employed to cut the reservoir in conjunction with the DFN.

A series of works have demonstrated the validation of the method for fully coupled hydra-mechanical simulations and successfully validated it with analytical solutions (Dontsov & Zhang 2018; Zhang et al. 2020; Chang & Hou 2023). This study introduces heat distribution calculations, where interactions between physical fields are considered to capture the dynamics between temperature changes, stress redistribution, and fluid movement. Fig. 1 shows the THM coupling process of this model, where the hydro-mechanical calculation is fully coupled and sequentially coupled with the thermal calculation.

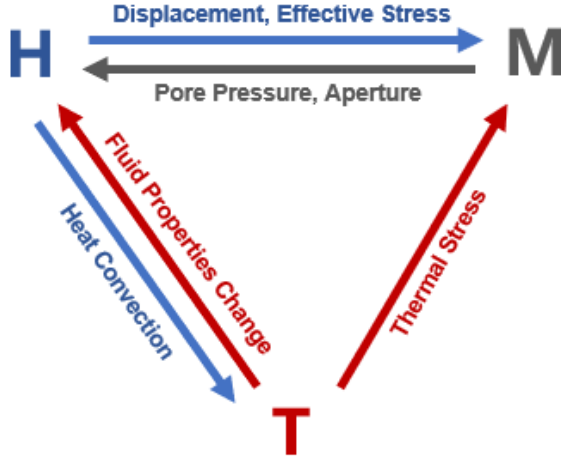


Fig. 1 THM coupling process in the model

2.2 Governing equations

The thermal calculations consider the transient conduction of heat within the rock mass, within the fluid, and between the rock and the fluid, respectively. The energy balance equation forms the basis for the energy distribution and temperature evolution within the rock mass, which could be expressed as:

$$\nabla \cdot q_s^T + q_v + A_s h (T_f - T_s) = \rho_s C_s \frac{\partial T_s}{\partial t} \quad (1)$$

Where	q_s^T	Specific heat flux of rock
	q_v	Volumetric heat source term
	A_s	Contact area per unit volume of rock
	h	Fluid-rock heat transfer coefficient
	ρ_s	Density of rock
	C_s	Specific heat of rock
	t	Time
	T_s	Temperature of rock
	T_f	Temperature of fluid

The specific heat flux is quantified using Fourier's Law, which relates the heat flux to the negative gradient of temperature:

$$q_s^T = -k^s \Delta T_s \quad (2)$$

Where k^s Thermal conductivity of rock

In the model, thermal effects lead to mechanical deformation primarily through thermal expansion, inducing thermal strains in the material that are integrated into the stress-strain relationship. The thermal stress is added to the zone stress state prior to the application of the mechanical constitutive law:

$$\Delta \sigma_{ij} = \delta_{ij} \cdot (-3K\alpha_t \Delta T) \quad (3)$$

$$\rho_f C_f \frac{\partial T_f}{\partial t} + \nabla \cdot q_f^T + \rho_f C_f q_f^f \cdot \nabla T_f + A_f h (T_f - T_s) = 0 \quad (4)$$

Where	$\Delta \sigma_{ij}$	Stress change due to thermal expansion or contraction
	K	Bulk modulus of rock
	α_t	Linear thermal expansion coefficient of rock
	δ_{ij}	Kronecker delta

Thermal convection in fluid is implemented by incorporating the advective component of heat transport, where the fluid movement contributes to changes in temperature distribution within the system. The rate of heat transport within the fluid flow is represented by:

$$q_f^T = -k_f^T \nabla T \quad (5)$$

Where q_f^T Specific heat flux of fluid
 k_f^T Fluid thermal conductivity

2.3 Model setup

A model is created based on the real data from the Gonghe basin. As shown in Fig. 2 a), the external size of the model is $200 \text{ m} \times 200 \text{ m} \times 200 \text{ m}$, with a core DFN region of $100 \text{ m} \times 200 \text{ m} \times 200 \text{ m}$. A Young's modulus of 43 GPa, Poisson's ratio of 0.21, tensile strength of 11 MPa, and density of 2600 kg/m^3 were used for the intact rock properties of granite.

The specific heat capacity of granite is set to $790 \text{ J/kg} \cdot ^\circ\text{C}$, the thermal conductivity is $2.4 \text{ W/m} \cdot ^\circ\text{C}$, and the coefficient of thermal expansion is $5.4 \times 10^{-6} \text{ } ^\circ\text{C}^{-1}$. Fluid property changes are calculated in accordance with the IAPWS formulation, which primarily considers the update of the fluid viscosity in this model (Huber et al. 2009). The initial temperature of the reservoir and the injected fluid are set to 200°C and 30°C , respectively.

A series of simplification measures are applied to ensure the mesh quality of the model and the convergence of the numerical calculations (Du et al. 2024). Ultimately, three major groups of natural fractures are considered based on the field drilling data, as illustrated in the stereonet in Fig. 2 b). The total number of fractures is 122, with the size following a power-law distribution, from 20 m to 40 m.

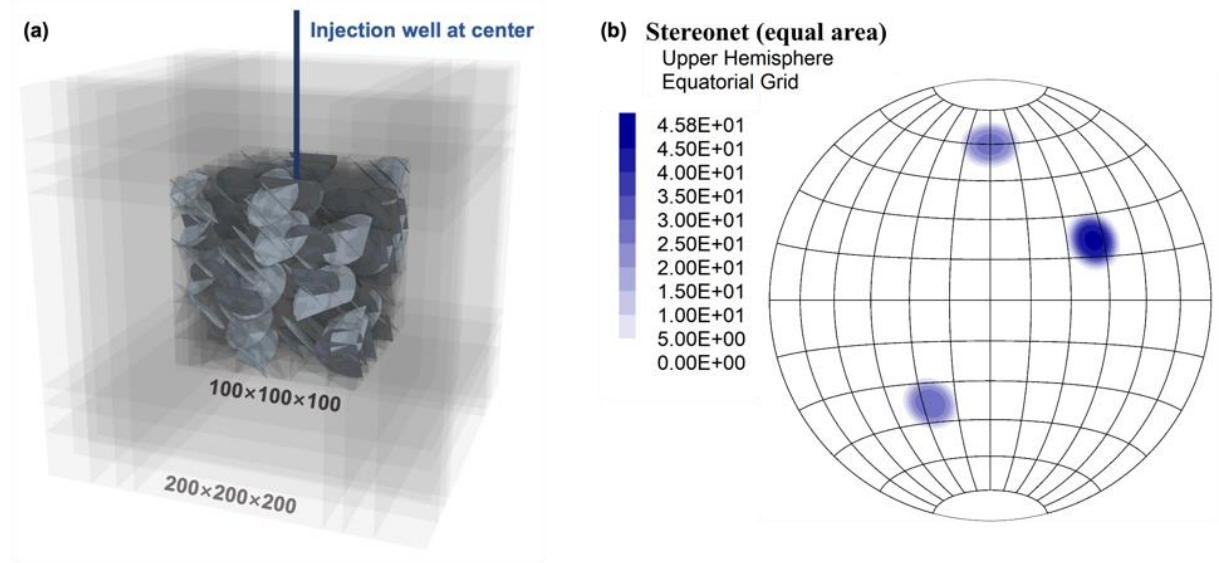


Fig. 2 a) The whole region and the core region with DFN and b) DFN stereonet of the model

3 Numerical result

The impact of heat evolution on hydraulic fracturing can facilitate comprehension of the mechanism through which fluids interact with various reservoir components, thereby enabling the design and optimization of injection methods. This section presents the results of THM-coupled simulations and subsequently compares the damage characteristics of reservoir fractures before and after considering thermal effects, to analyze the mechanism through which cold water injection affects fracturing.

3.1 Temperature distribution

Fig. 3 shows the fluid temperature distribution over the whole fracture network and the main fracture surface, respectively. In this case, the initial temperature of the reservoir is 200°C and the injected fluid is set to 30°C . The model is capable of stable numerical calculation and simulation of transient

flow and heat transfer. After a 2000 s injection, the cold fluid diffused in the fracture network and the temperature gradually increased as it moved away from the injection point.

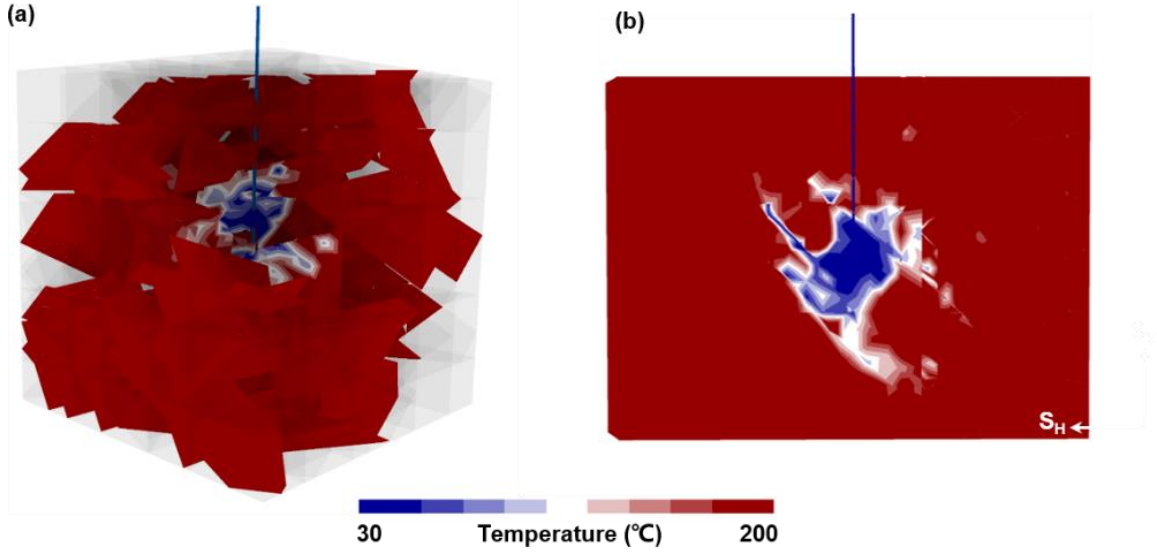


Fig. 3 Temperature distribution after injection: a) The fracture network; b) The main fracture plane

Fig. 4 illustrates the variation in average fluid temperature over time. The average temperature of the fluid within the fractures increases gradually as a consequence of the heating effect of the rock body and fluid diffusion over time. In particular, the average temperature of natural fractures is approximately 50% higher than that within the main fracture. This is because the natural fracture is relatively further away from the injection location while having a larger contact area with the rock.

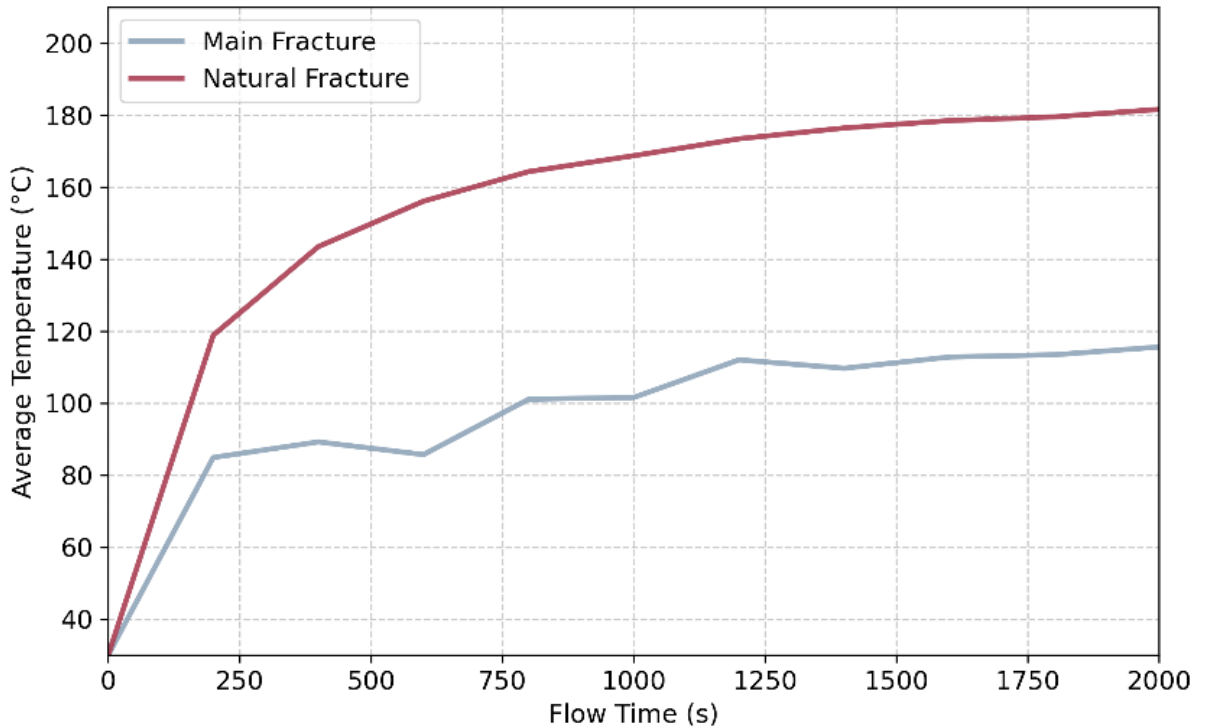


Fig. 4 Temperature variation in main and natural fractures

3.2 Comparison of THM and HM coupled results

A hydro-mechanical coupling simulation was conducted to compare with the results of the THM model, to show the influence of thermal effects on hydraulic fracturing. The HM model was configured with a fluid property of 30°C, while the remaining injection conditions were the same. Fig. 5 shows a vertical view of the fracture network of the two models. After the same injection time, the fracture network morphology in both models shows a similar trend, i.e., natural fractures dominate the

whole fracture network. This also matches our previous findings. In comparison, the THM model exhibits greater fracture concentration, while the HM model is slightly more extensive.

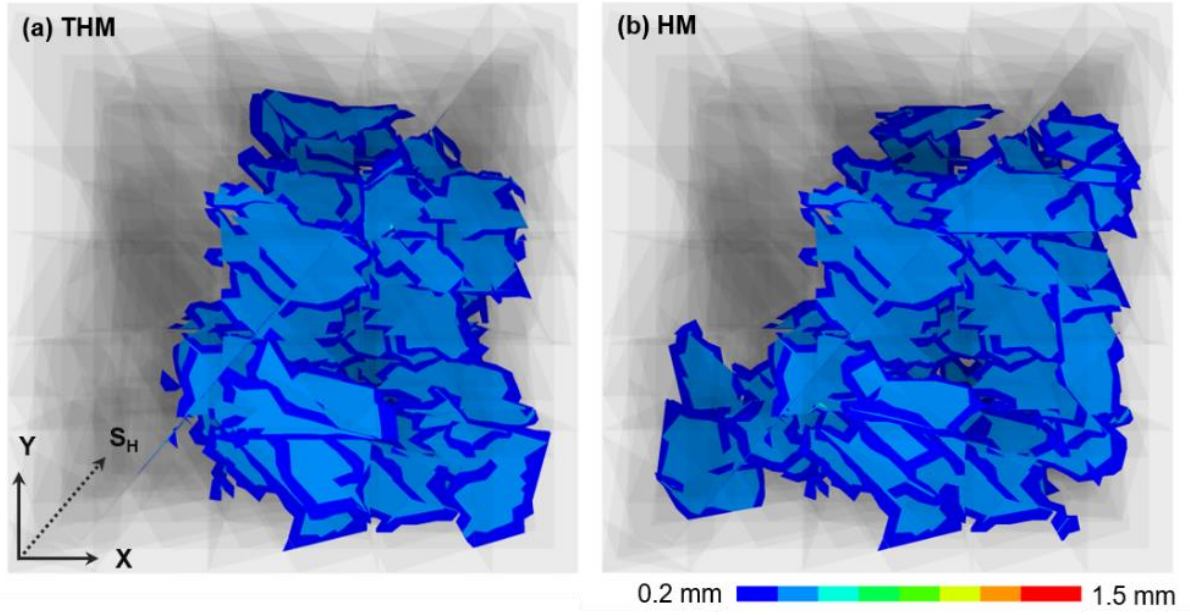


Fig. 5 Vertical view of the total fracture network

The double y-axis plots in Fig. 6 illustrate the temporal variation of the damaged fracture area. The line and area plots respectively reflect the total damaged fracture area and the difference between the fracture areas of the two models. The results demonstrate that the growth trend of the area of the two models is similar, but the change in the area difference exhibits an inverse trend. The area of the THM model is dominant in the pre-injection period and is surpassed by the HM model in the middle period. This indicates that the fracture destruction rate of the THM model is faster in the pre-injection period, but begins to slow down gradually after a period of time.

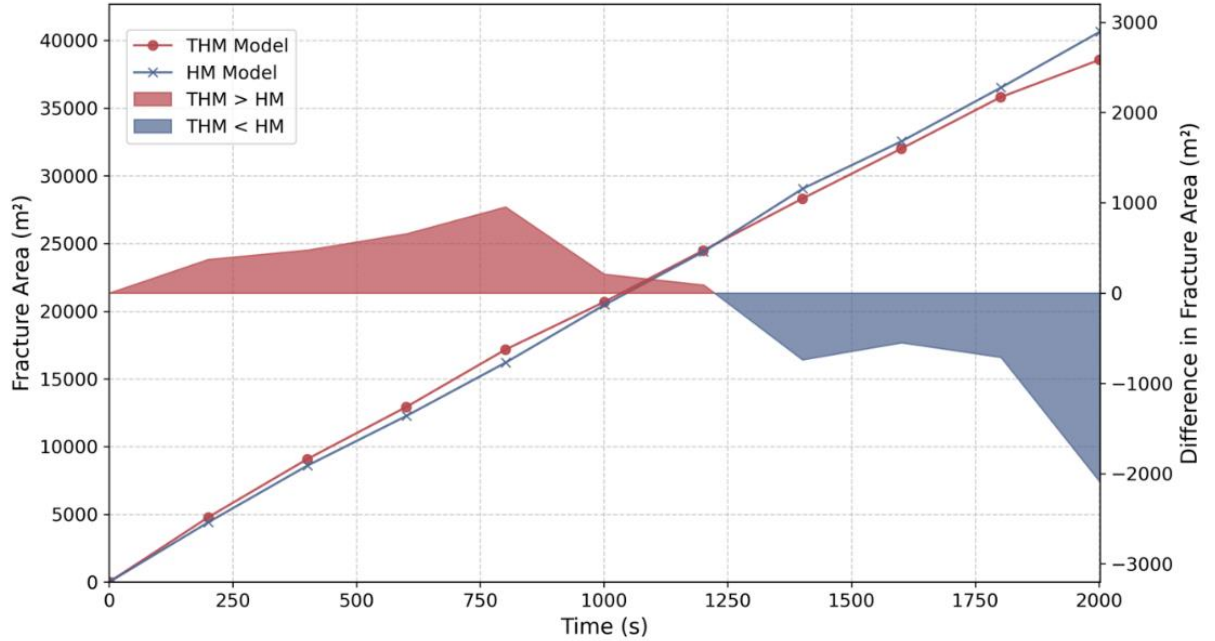


Fig. 6 Variation of fracture area with time (the left y-axis corresponds to a line plot, the right y-axis is an area plot reflecting the difference in fracture area between the two models)

This trend also reveals the mechanism of thermal influence on fracture expansion. In the early stage of fracturing, the injection of cold water rapidly reduces the temperature of the rock near the borehole. The rock on both sides of the fracture face shrinks linearly and resists part of the compressive stress. The strength of the fracture is weakened, thereby increasing the rate of its initiation and expansion.

However, as the fracturing progresses, the average temperature of the fluid gradually increases (as shown in Fig. 3). This phenomenon is more pronounced at the tip of the fracture due to its distance from the injection point and continuous heating. The temperature difference between the fluid and the surrounding rock is reduced, and the temperature of the rock is less likely to be lowered, thus the fracture extension rate is no longer accelerated.

Also, increased temperatures markedly diminish the viscosity of the fluid. The ultra-low viscosity fluid, despite exhibiting enhanced penetration properties, displays a diminished capacity for fracture initiation and support. This is also evident in the reduced seam width of the overall network of seams, which averages 0.7 mm. Consequently, the rate of fracture expansion in the THM model is markedly constrained in the middle and late fracturing stages due to the dual effects of lower viscosity and higher temperature.

The influence of temperature and viscosity on fracture propagation provides a basis for optimizing injection strategies. Increasing fluid viscosity during the early and middle stages of hydraulic fracturing facilitates the propagation of primary fractures and mitigates the adverse effects of low-viscosity fluids. In contrast, reducing fluid viscosity in the later stages of fracturing enhances the activation of natural fractures and improves fluid permeability. Additionally, increasing the injection rate in the final stages promotes the thermal cracking of the rock, further improving stimulation efficiency.

4 Conclusion

This study introduces a new thermal-hydro-mechanical coupled simulation method based on distinct element method for temperature-related fluid transport modelling in fractured rock. Heat conduction and convection are considered in the model where DFN is explicitly represented, and fluid properties are updated with temperature and pressure.

The hydraulic fracturing process was simulated using THM and HM coupling, respectively. The average temperature of the fluid inside the fracture gradually increases with time and fluid diffusion. The rate of fracking in the THM model is faster in the early stage due to the cold water injection that promotes rock initiation. However, its ultimate fracture area is eventually smaller than the HM model due to the increase in temperature and decrease in viscosity.

Elevating fluid viscosity during the post stages of fracturing helps in the extension of the main fracture and mitigates the negative effects of low-viscosity fluids. This THM method can be further used to simulate the real response of the reservoir and for designing more optimized injection strategies.

References

- Chang Z, Hou B (2023) Numerical simulation on cracked shale oil reservoirs multi-cluster fracturing under inter-well and inter-cluster stress interferences. *Rock Mechanics and Rock Engineering* 56: 2253–2270. <https://doi.org/10.1007/s00603-022-03145-7>
- Dontsov EV, Zhang F (2018) Calibration of tensile strength to model fracture toughness with distinct element method. *International Journal of Solids and Structures* 144: 180–191. <https://doi.org/10.1016/j.ijsolstr.2018.05.001>
- Du B, Zhang F, Zhang C (2024) Distinct element modeling of hydraulic fracture propagation with discrete fracture network at Gonghe enhanced geothermal system site, northwest China. *Journal of Rock Mechanics and Geotechnical Engineering*. <https://doi.org/10.1016/j.jrmge.2024.04.028>
- Huber ML, Perkins RA, Laesecke A, Friend DG, Sengers JV, Assael MJ, Metaxa IN, Vogel E, Mareš R, Miyagawa K (2009) New international formulation for the viscosity of H₂O. *Journal of Physical and Chemical Reference Data* 38:101–125. <https://doi.org/10.1063/1.3088050>
- Itasca (2016) 3DEC—3-Dimensional Distinct Element Code, User's Guide. Itasca Consulting Group Inc., Minneapolis, Minnesota.
- Li J, Chen S, Yang F, et al. (2024) Experimental study of hydraulic properties of the granite fracture under heating-cooling cycles. *International Journal of Heat and Mass Transfer* 220: 125003. <https://doi.org/10.1016/j.ijheatmasstransfer.2023.125003>

- Liao J, Hu K, Mehmood F, et al. (2023) Embedded discrete fracture network method for numerical estimation of long-term performance of CO₂-EGS under THM coupled framework. *Energy* 285: 128734. <https://doi.org/10.1016/j.energy.2023.128734>
- Liu Y, Zhang F, Weng D, et al. (2024) Two-phase flow thermo-hydro-mechanical modeling for a water flooding field case. *Rock Mechanics Bulletin* 3(3): 100125. <https://doi.org/10.1016/j.rockmb.2024.100125>
- Riahi A, Pettitt W, Damjanac B, Varun (2019) Numerical modeling of discrete fractures in a field-scale FORGE EGS reservoir. *Rock Mechanics and Rock Engineering* 52: 4229–4246. <https://doi.org/10.1007/s00603-019-01894-6>
- Schimmel M, Liu W, Worrell E (2019) Facilitating sustainable geo-resources exploitation: A review of environmental and geological risks of fluid injection into hydrocarbon reservoirs. *Earth-Science Reviews* 192: 455–475. <https://doi.org/10.1016/j.earscirev.2019.01.015>
- Xue Y, Liu S, Chai J, Liu J, Ranjith PG, Cai C, Gao F (2023) Effect of water-cooling shock on fracture initiation and morphology of high-temperature granite: Application of hydraulic fracturing to enhanced geothermal systems. *Applied Energy* 332: 120019. <https://doi.org/10.1016/j.apenergy.2023.120858>
- Yuan B, Wood DA (2018) A holistic review of geosystem damage during unconventional oil, gas and geothermal energy recovery. *Fuel* 225: 108–132. <https://doi.org/10.1016/j.fuel.2018.03.091>
- Zhang S, Yan W, Li D, et al. (2018) Characteristics of geothermal geology of the Qiabuqia HDR in Gonghe Basin, Qinghai Province. *Chinese Geology* 45: 1087–1102. <https://dx.doi.org/10.12029/gc20180601>
- Zhang F, Yin Z, Chen Z, Maxwell S, Zhang L, Wu Y (2020) Fault reactivation and induced seismicity during multistage hydraulic fracturing: Microseismic analysis and geomechanical modeling. *SPE Journal* 25: 692–711. <https://doi.org/10.2118/199883-PA>
- Zhang C, Fan D, Elsworth D, et al. (2024) Mechanisms of stress-and fluid-pressure-driven fault reactivation in Gonghe granite: Implications for injection-induced earthquakes. *International Journal of Rock Mechanics and Mining Sciences* 174: 105642. <https://doi.org/10.1016/j.ijrmms.2023.105642>